frontiers | Frontiers in Mechanical Engineering

ORIGINAL RESEARCH
published: 06 June 2022
doi: 10.3389/fmech.2022.884111

# Analytical Study on Time-Dependent Stiffness of Stud Shear Connectors

*Rong Liu*[1]*, *Xinyang Sun*[1], *Hengda Ye*[1] and *Yuqing Liu*[2]

[1]College of Civil and Transportation Engineering, Hohai University, Nanjing, China, [2]Full Professor, Department of Bridge Engineering, Tongji University, Shanghai, China

Concrete creep weakens the spring stiffness of stud shear connectors (SSCs) and increases the long-term deflection of long-span composite beams. The time-dependent properties of SSC are of great importance for the long-term evaluation of composite steel construction. This paper proposes the time-dependent stiffness (TDS) method based on the analytical solution of the beam on a viscoelastic foundation to simulate the SSC under the sustained push-out load. TDS method combines beam theory and the viscoelastic property of hardened concrete. The long-term slip of SSC is predicted by hand calculation of the explicitly expressed governing equation, and it is close to the refined finite element analysis (FEA) results. The constants and parameters used to determine TDS seem to be insensitive regarding geometric and material variation. TDS may provide a simplified method to incorporate the time-dependent partial interaction into complex composite structures by saving the consumption of computer storage and advanced modeling time which are usually required in the refined modeling at the steel-concrete interface, especially when the long-term properties of concrete are of interest.

**Keywords: stud shear connector, long-term behavior, shear stiffness, aging coefficient, beams on Winkler foundations**

OPEN ACCESS

***Edited by:***
*Denis Benasciutti,*
*University of Ferrara, Italy*

***Reviewed by:***
*Ali Nikkhoo,*
*University of Science and Culture, Iran*
*Frédéric Charles Lebon,*
*Aix-Marseille Université, France*

***Correspondence:**
*Rong Liu*
*liurong1983@hhu.edu.cn*

***Specialty section:***
*This article was submitted to Solid and Structural Mechanics, a section of the journal Frontiers in Mechanical Engineering*

***Received:*** *25 February 2022*
***Accepted:*** *16 May 2022*
***Published:*** *06 June 2022*

***Citation:***
*Liu R, Sun X, Ye H and Liu Y (2022) Analytical Study on Time-Dependent Stiffness of Stud Shear Connectors. Front. Mech. Eng 8:884111. doi: 10.3389/fmech.2022.884111*

## INTRODUCTION

SSC is the most widely used connectors for composite steel construction owing to its isotropic shear performance in the shear plane, mature and convenient welding technology, and stable quality assurance (AASHTO, 2012). When considering the creep and shrinkage characteristics of concrete, under the long-term constant load, the deformation of the steel-concrete composite structure will increase with the development of time, which will affect the normal service performance of the structure. Gilbert and Bradford (1991) conducted an experimental study on the time-dependent behavior of steel-concrete simply supported composite beams under long-term constant load. The results show that the long-term deformation of composite beams with concrete creep shrinkage for 250 days is about twice the initial deformation. The concrete creep is significant for the long-term behavior of composite beams. To predict the long-term behavior of composite beams, Al-Deen et al. (2011) and Ban et al. (2015) conducted FEA using spring elements to represent the SSCs at the steel-concrete interface. Without considering the slip at the interface, the deformation of the beam may be underestimated. Al-Deen et al. (2011) also conducted a long-term push-out test of SSC. The test results showed that under the long-term constant sustained push-out load, the relative slip after 432 days is approximately twice of the instantaneous slip. It indicates that the stiffness of SSC decreases with the increase of loading time. Mirza and Uy (2010) conducted a finite element analysis of the long-term push-out test of SSC used in composite slab with profiled steel sheets. The results showed that the ultimate resistance and the stiffness of SSC decreased with the development of time.

Liu et al. (2020a) reported the stress redistribution of the long-term loaded studs with the great increase of local stress concentration at the shank-plate weld toes. Concrete creep plays as an important role for the stress concentration of SSC. Generally, local stress concentration may decrease the fatigue resistance of SSC (Liu et al., 2020b). It implies that the concrete creep may have influence on the fatigue behavior of SSC. For concrete creep, numerous models have been applied to predict the long-term behavior (Liu et al., 2021). Besides the concrete elements, the anchorage concrete of connectors may enlarge the long-term effects. A constant shear stiffness cannot predict either the shear force or the slip of the connector (Liu et al., 2020c). Limited researches have been carried out to clarify the long-term behavior of SSC, though the time-dependent material properties of concrete may not only affect the concrete components but also the steel-concrete inter connection, considering the slip increase, ultimate strength reduction, and the stress redistribution potentially deteriorating its fatigue resistance. This paper focus on how to predict the time-dependent slip of SSC using the analytical approach.

Considering the tedious time consumption of long-term tests and the experience-based refined FEA application, hand calculation of SSC is of interest in design application. Lots of tests have been conducted to determine the short-term shear stiffness of SSC. Semi-empirical equations representing the load-slip curve (Xue et al., 2008) or secant shear stiffness of SSC (Lin et al., 2014) have been proposed. However, few studies on TDS of SSC have been conducted. Al-Deen et al. (2011) used the age adjusted effective stiffness (AAES) of SSC, as shown in **Eq. 1**, to simulate the time-dependent behavior of composite beams.

$$K_e(t,\tau) = \frac{K_{\text{ini}}(\tau)}{1 + \chi_{\text{sc}}(t,\tau)\varphi_{\text{sc}}(t,\tau)} \tag{1}$$

Where, $K_e(t, \tau)$ is the effective stiffness of SSC adjusted according to the load age $\tau$ and loading time $t$. $K_{\text{ini}}(\tau)$ is the shear stiffness of SSC at the loading age $\tau$. It is equivalent to the initial instantaneous shear stiffness. $\chi_{\text{sc}}(t, \tau)$ is the aging coefficient of SSC. It is 0.75 for primary loads and 0.55 for imposed secondary loads like shrinkage. $\varphi_{\text{sc}}(t, \tau)$ is the creep coefficient of the connector, and it is proportional to the concrete creep coefficient $\varphi_c(t, \tau)$, as shown in **Eq. 2**.

$$\varphi_{\text{sc}}(t,\tau) = \alpha_{\text{sc}}\varphi_c(t,\tau) \tag{2}$$

Where, $\alpha_{\text{sc}}$ is determined according to the long-term push-out test results of SSC. Al-Deen et al. (2011) set $\alpha_{\text{sc}}$ as a constant value of 0.4 without mathematical explanation or parametric test calibration. Ban et al. (2015) also used **Eq. 1** to determine TDS of SSC without further investigation of $\alpha_{\text{sc}}$. Since few tests of long-term loaded SSC are available, analytical study of SSC under sustained loading is of urgent to provide reasonable solution and reliable parameters for TDS. The analytical solution of TDS for SSC with variable geometric parameters and time-dependent material properties of concrete has not been obtained yet.

Analytical study of SSC under short-term push-out load might be idealized and simplified as the beam on elastic foundation

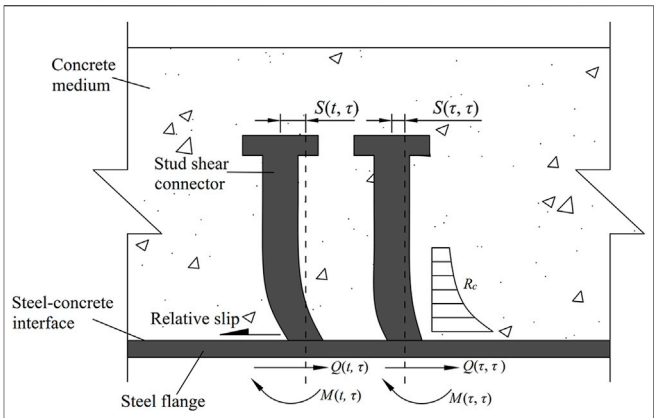


**FIGURE 1 |** Long-term deformation of stud shear connector.

which yielded analytical solution (Winkler, 1867). Many scholars have carried out theoretical research on the deformation and stress of SSC based on the elastic foundation beam theory. Slutter (1966) explored the deflection equations under concentrated shear force and concentrated bending moment. Gelfi and Giuriani (1987) simplified the differential equations based on the displacement boundary condition of the infinite beam, and deduced the deflection of SSC and the corresponding initial shear stiffness. Akao et al. (1987) assumed that the rotation of SSC was limited, and derived the deflection expression of SSC using the beam on elastic foundation theory. Lin et al. (2014) used the initial parameter to solve the differential equation of the finite-length beam, and deduced the expression of the initial shear stiffness of SSC. Push-out test results were analyzed to determine the equation of short-term shear stiffness. Xu and Liu (2016) deduced the initial shear stiffness equation of SSC covered by rubber sleeves. However, all of these analytical studies assume that the soil springs of the elastic foundation exhibit constant modulus of subgrade reaction or spring stiffness. However, considering the viscoelastic behavior of concrete creep, the spring stiffness of the foundation is time-dependent and it is affected at least by the loading age, loading time, and the push-out load. Thus, the previous analytical solutions of SSC under push-out loads have not covered the long-term behavior of SSC and further research is needed.

This paper aims to derive the analytical solution of TDS for SSC under long-term loading. We introduce the viscoelastic creep properties of the foundation by using the time-dependent spring stiffness to improve the available beam on elastic foundation theory with constant settlement stiffness. The proposed equation is checked with FEA results and available equations to calibrate its accuracy. The parameters, like stud geometry, concrete strength, cure age and load time, are examined to check the sensitivity of TDS. Compared with previous researches, the major difference of this paper is the analytical solution of TDS. It is obtained *via* the combination of the beam on elastic foundation and concrete creep after introducing two additional arguments curing age $\tau$ and loading age $t$ into the governing equations. The solution yields improved analytical accuracy considering the geometric and material variation.

# ANALYTICAL MODEL OF STUD UNDER SUSTAINED PUSH-OUT LOAD

## Conception of Time-Dependent Shear Connectors

As shown in **Figure 1**, SSC combined with the steel beam and the concrete slab is mainly used to bear the shear force on the interface and transmit it to the compressed concrete in contact with SSC. SSC and the concrete are within the local range of the shank. Additional deformation occurs, causing relative slip at the steel-concrete interface. As the age of concrete increases, the compressive concrete on the stud foot undergoes creep deformation under the action of local stress. During the deformation process, SSC and the compressed contact surface of the concrete are always in close contact, resulting in an increase in the deformation of SSC and the relative slippage of the interface. With the increase of loading time, in the long run, the interface between steel and concrete may cause combined damage, concrete cracking and other deterioration. The long-term slippage of the interface is related to the material and cross-sectional properties of the stud and the material properties of the concrete. The long-term shear resistance of the stud depends on the combined action of the concrete and the stud. In the theoretical analysis of the time-dependent behavior of SSC, the elastic foundation beam theory that can consider the concrete deformation is adopted. At this time, SSC and the concrete of the hole wall can be compared as a local elastic foundation beam. For the creep problem of concrete in the normal use stage, it is generally based on the linear creep theory analysis. At this time, it is considered that both steel and concrete materials are in the elastic stress range. The effective modulus $E_c$ $(t,\tau)$ adjusted according to the age is used to replace the initial elastic modulus $E_c$ $(\tau)$ of concrete, and the creep deformation is included in the elastic deformation. The calculation is simple and the accuracy is high. This idea is introduced into the beam model of elastic foundation, and the influence of creep of concrete foundation on beam deformation and mechanical performance can be analyzed.

## Basic Assumptions

In order to simplify the theoretical derivation of TDS of SSC, the following reasonable assumptions are made according to the long-term stress mechanism of welding studs: 1) The deformation of SSC section conforms to the assumption of the plane section; 2) During the creep period, the concrete is regarded as the Winkel foundation, and the shear deformation is ignored; 3) Concrete and steel are regarded as elastic homogeneous materials during creep; 4) The axial force of SSC and the friction force of the contact surface with the concrete are ignored; 5) During the creep period, SSC and the concrete compression contact surface are always in close contact.

## Governing Differential Equations

The original theory of beam on elastic foundation is shown in **Eq. 3a** (Winkler, 1867). The pressure $p$ over the $x$-$y$ plane results in vertical deflection $w$ with the constant spring stiffness $k$.

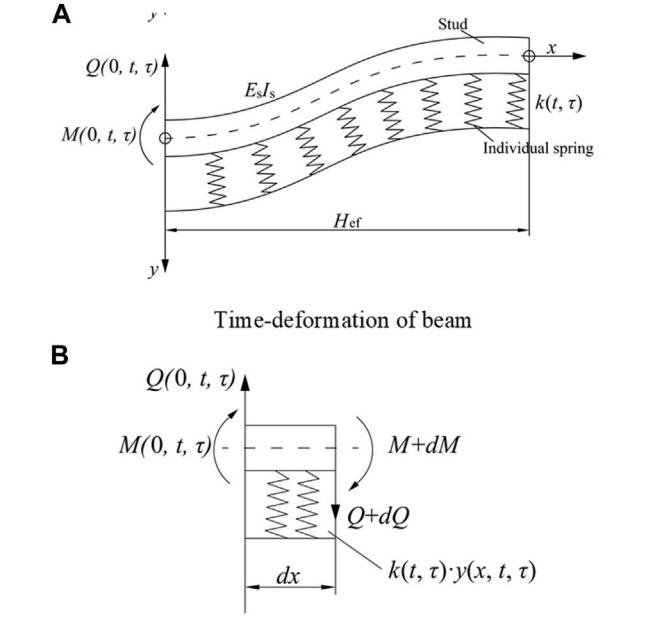


**FIGURE 2 |** Concepts of a beam on viscoelastic foundation.

$$p(x, y) = k \cdot w(x, y) \tag{3a}$$

Utilizing the theory of beam on elastic foundation, the SSC embedded in concrete blocks is simplified as **Eq. 3b** (Lin et al., 2014). Where, $R$ is the reaction force, $y$ is the deflection.

$$R(x) = k \cdot y(x) \tag{3b}$$

To include the concrete creep effects, the reaction force and the deflection should be time-dependent with varying loading duration $t$-$\tau$. Thus, two new arguments, the concrete curing age $\tau$ and the loading time $t$, are introduced. Besides, the spring stiffness should not be constant since the concrete creep shows both strain-dependent and stress-dependent behavior. Improving **Eq. 3b** with the time-dependent material properties, this paper develops the governing equations of SSC under sustained loading.

**Figure 2A** shows the force mode of the push-out test stud connector, the stud diameter $d_s$, the height $h_s$, the elastic modulus $E_s$, and the bending moment of inertia $I_s$. Taking the centroid of the root section of the welding nail as the origin, the longitudinal direction of the shank is the $x$-axis, and the vertical direction is the $y$-axis, and a rectangular coordinate system is established.

The root of SSC bears the vertical concentrated shear force $Q_0$ $(t, \tau)$ at the age t, the reaction moment $M_0$ $(t, \tau)$ is generated by the constraint of the steel beam flange plate, and the reaction force $R$ $(x, t, \tau)$, the load of the rest of SSC is basically 0, which is not considered in the analysis. During creep, the reaction force $R$ $(x, t, \tau)$ of the concrete foundation at any point along the longitudinal direction of the shank is proportional to the deformation y (x, t, τ) at that point, that is,

$$R(x,t,\tau) = k(t,\tau)\cdot y(x,t,\tau) = k_e(t,\tau)\cdot b\cdot y(x,t,\tau) \quad (3c)$$

In **Eq. 3c**, $\tau$ is the loading age; $k$ ($t$, $\tau$) is the foundation constant or Winkel constant, in MPa, and $k$ ($t$, $\tau$) is a constant in the concrete foundation with age $t$; $k_e$ ($t$, $\tau$) is the effective modulus of the concrete foundation during creep, in MPa/mm; $b$ is the transverse effective distribution width of SSC, and $b$ is about $0.8d_s$. Gelfi and Giuriani (1987), Lin et al. (2014), Zheng and Liu (2014) and others believed that the modulus of concrete foundation is proportional to the elastic modulus. After considering the creep effect of concrete, the age-adjusted effective modulus method (AEMM) proposed by Bazant (1972) was used to adjust the modulus of concrete foundation at the loading age $\tau$, then the effective modulus of the concrete foundation at the loading time $t$ is:

$$k_e(t,\tau) = \frac{k_0(\tau)}{1+\psi_c(t,\tau)\cdot\varphi_c(t,\tau)} \quad (4)$$

In **Eq. 4**, $k_0$ ($\tau$) is the modulus of concrete foundation at the initial stage of loading; $\psi_c$ ($t$, $\tau$) is the aging coefficient of concrete; $\varphi$ ($t$, $\tau$) is the creep coefficient of concrete.

The differential element of elastic foundation beam with interception length d$x$ is used to establish the equilibrium differential equation, as shown in **Figure 2B**. The specified shear force $Q$ ($x$, $t$, $\tau$) makes the element rotate clockwise and the section bending moment $M$ ($x$, $t$, $\tau$) makes the element pull-down and upward pressure positive, and the supporting reaction force $R$ ($x$, $t$, $\tau$) points to the element is positive. Taking the loading time $t$ as an example, according to the vertical equilibrium of the internal force of the element and the moment equilibrium of the right end of the element, we can get:

$$\frac{dQ(x,t,\tau)}{dx} = k(t,\tau)\cdot y(x,t,\tau) \quad (5)$$

$$Q(x,t,\tau) = \frac{dM(x,t,\tau)}{dx} \quad (6)$$

Substitute **Eq. 6** into **Eq. 5** to get:

$$\frac{dQ(x,t,\tau)}{dx} = \frac{d^2M(x,t,\tau)}{dx^2} = k(t,\tau)\cdot y(x,t,\tau) \quad (7)$$

Using the differential equation of beam flexural deformation and substituting into **Eq. 7**, the equilibrium differential equation of the elastic foundation beam is obtained:

$$-E_sI_s\frac{d^4y(x,t,\tau)}{dx^4} = k(t,\tau)\cdot y(x,t,\tau) \quad (8)$$

**Equation 8** can also be rewritten as a fourth-order constant coefficient homogeneous differential equation:

$$\frac{d^4y(x,t,\tau)}{dx^4} + 4\alpha(t,\tau)\cdot y(x,t,\tau) = 0 \quad (9)$$

Where, $\alpha$ ($t$, $\tau$) is called the characteristic coefficient, and its value depends on the ratio of the foundation constant $k$ ($t$, $\tau$) to the flexural stiffness $E_sI_s$ of the beam section, and the dimension is $(\text{length})^{-1}$, for the convenience of notation, and $\alpha$ ($t$, $\tau$) is uniformly represented by $\alpha$ below.

The general solution of homogeneous **Eq. 9** is:

**TABLE 1 |** Classification of beams on elastic foundations considering creep.

| Types | Loading age τ | Creep time *t* |
|---|---|---|
| I | Long | Long |
| II | Long | Moderate |
| III | Moderate | Moderate |

$$y(x,t,\tau) = e^{-\alpha x}[A_1\cos\alpha x + A_2\sin\alpha x] + e^{\alpha x}[A_3\cos\alpha x + A_4\sin\alpha x] \quad (10)$$

Where, $A_1$, $A_2$, $A_3$, and $A_4$ are integral constants, and their values are determined according to the known boundary conditions.

## Boundary Conditions

The relative stiffness of the beam and the foundation has an important influence on the stress state of the foundation beam. The relative stiffness is generally characterized by the characteristic length αhs. According to the value of αhs, the beams can be divided into the following three categories (Hetenyi, 1958):

1) Short beam: $\alpha h_s < \pi/4$, the bending deformation of the beam is very small compared with the deformation of the foundation. In most cases, the bending deformation of the beam can be ignored, and the beam can be considered to be absolutely rigid at this time.
2) Moderate beams: $\pi/4 \le \alpha h_s \le \pi$, the load acting on one end of the beam has limited influence on the other end and cannot be ignored. In this case, it is necessary to use the initial parameter method to accurately calculate the deformation and force of the beam.
3) Long beam: $\alpha h_s > \pi$, the displacement and force at both ends of the beam do not affect each other. When studying the force and deformation at one end of the beam, it can be assumed that the other end of the beam is infinite. According to the distance between the load and the beam ends, it can be divided into are infinitely long beams and semi-infinitely long beams.

In construction and bridge engineering, the commonly used SSC are generally 10–30 mm in diameter, 50–400 mm in length, and the concrete strength is between C15–C70 (Lin et al., 2014). The calculated characteristic length $\alpha h_s$ is greater than $\pi/4$. Therefore, SSCs for engineering are generally calculated as medium-long beams or long beams. The deformation of the foundation and the beam are considered in the calculation of these two types of beams, and there is no difference in essence. The influence of the boundary conditions at both ends on the beam deformation and internal force is relatively complicated to calculate, but the calculation accuracy of the deformation and internal force at the right end of the beam is high. If the foundation beams are strictly classified according to $\alpha h_s$, the foundation becomes soft after considering the creep effect of concrete. Taking 10 years of creep as an example, the supporting stiffness $k_e$ of the foundation is generally reduced to 30%–60% of the initial loading, and the corresponding characteristic length $\alpha h_s$ Reduced, there may be three cases of changes in the type of foundation beams as shown in **Table 1**. In the mathematical derivation, it needs to be classified and discussed according to the change of the foundation beam type, and the derivation is

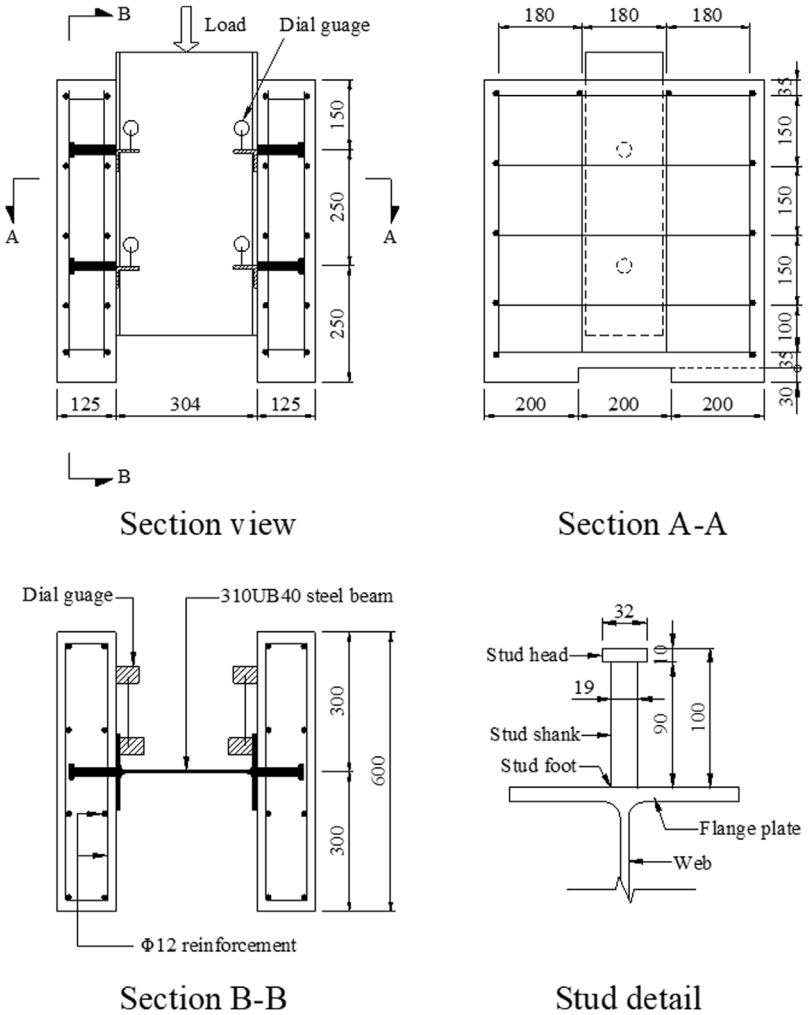


**FIGURE 3 |** Structural details of the push-out specimen (unit: mm).

cumbersome and of little significance. Aiming at the limited length of SSC, this paper adopts the initial parameter method to theoretically deduce according to the type of moderate and long beams.

When Lin et al. (2014) and Xu and Liu (2016) derived the expression of the initial shear stiffness of SSC, for SSC connector with $\alpha h_s \geq 5$, it is considered that the deflection and rotation angle of the top of SSC are basically 0, that is, the right end of the foundation beam is completely consolidated. The deformation capacity of SSC is characterized according to the deflection of the beam root. When the concrete undergoes time-dependent deformation, the boundary conditions at the ends of SSCs change continuously with age. It is very complicated to calculate the long-term deformation of SSCs precisely. It is necessary to simplify the boundary conditions of the foundation beam model during creep. According to the long-term stress mechanism of SSC, the overall vertical slip of SSC in the concrete has little effect on the end force, and the bending deformation accounts for more than 80% of the relative slip of the steel-concrete interface, which is an important component of the interface slip. part. Therefore, it is reasonable and feasible to use the bending deformation to characterize the long-term deformation ability of SSC, assuming that the top of SSC is always consolidated during the creep period, and the rotational freedom of the root of SSC is completely constrained by the steel girder flange plate (assuming that the stiffness of the steel girder flange plate is infinite). The boundary conditions of the stud connectors in the push-out test during creep are simplified as follows:

$$\left.\begin{array}{ll} \theta_0(t) = 0, & Q_0(t) = -P \\ \theta_{h_s}(t) = 0, & y_{h_s}(t) = 0 \end{array}\right\} \tag{11}$$

Where, $P$ is the vertical shear force along the positive direction of the $y$-axis applied to the root of SSC; according to the four known boundary conditions of **Eq. 11**, the four integral constants $A_1$–$A_4$ in **Eq. 10** can be obtained.

## Solution of Equations

For the problem of moderate and long beams, the four integral constants $A_1$–$A_4$ are changed to the four parameters $y_0(t, \tau)$, $\theta_0(t,$

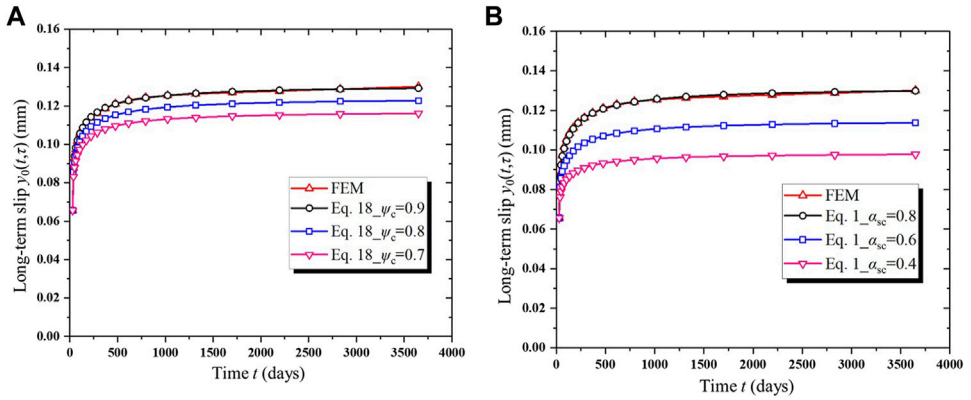


**FIGURE 4 |** Time-dependent slip predicted by analytical and FE methods.

$\tau$), $M_0(t,\tau)$, $Q_0(t,\tau)$. Introducing the hyperbolic function $sh\alpha x = \frac{e^{\alpha x}-e^{-\alpha x}}{2}$ and $ch\alpha x = \frac{e^{\alpha x}+e^{-\alpha x}}{2}$, **Eq. 10** is further rewritten as:

$$y(x,t,\tau) = ch\alpha x[B_1 \cos\alpha x + B_2 \sin\alpha x] + sh\alpha x[B_3 \cos\alpha x + B_4 \sin\alpha x] \tag{12}$$

Derivation of the above Eq. to find the initial parameters of the beam end point $O$:

$$\left.\begin{aligned} y(0,t,\tau) &= y_0(t,\tau) = B_1 \\ y'(0,t,\tau) &= \varphi_0(t,\tau) = \alpha\cdot B_2 + \alpha\cdot B_3 \\ y''(0,t,\tau) &= -\frac{M_0(t,\tau)}{E_sI_s} = 2\alpha^2\cdot B_4 \\ y'''(0,t,\tau) &= -\frac{Q_0(t,\tau)}{E_sI_s} = 2\alpha^3\cdot B_2 - 2\alpha^3\cdot B_3 \end{aligned}\right\} \tag{13}$$

Then the four integral constants $B_1$–$B_4$ are expressed as:

$$\left.\begin{aligned} B_1 &= y_0(t,\tau) \\ B_2 &= \frac{\varphi_0(t,\tau)}{2\alpha} - \frac{Q_0(t,\tau)}{4\alpha^3\cdot E_sI_s} \\ B_3 &= \frac{\varphi_0(t,\tau)}{2\alpha} + \frac{Q_0(t,\tau)}{4\alpha^3\cdot E_sI_s} \\ B_4 &= -\frac{M_0(t,\tau)}{2\alpha^2\cdot E_sI_s} \end{aligned}\right\} \tag{14}$$

Substitute **Eq. 14** into **Eq. 12** and reorganize:

$$y(x,t,\tau) = A(\alpha x)\cdot y_0(t,\tau) + B(\alpha x)\cdot\frac{\varphi_0(t,\tau)}{\alpha} - C(\alpha x)\cdot\frac{M_0(t,\tau)}{\alpha^2\cdot E_sI_s} - D(\alpha x)\cdot\frac{Q_0(t,\tau)}{\alpha^3\cdot E_sI_s} \tag{15}$$

In **Eq. 15**, A ($\alpha x$), B ($\alpha x$), C ($\alpha x$), D ($\alpha x$) are functions defined as follows:

$$\left.\begin{aligned} A(\alpha x) &= ch\alpha x\cdot\cos\alpha x \\ B(\alpha x) &= \frac{ch\alpha x\cdot\sin\alpha x + sh\alpha x\cdot\cos\alpha x}{2} \\ C(\alpha x) &= \frac{sh\alpha x\cdot\sin\alpha x}{2} \\ D(\alpha x) &= \frac{ch\alpha x\cdot\sin\alpha x - sh\alpha x\cdot\cos\alpha x}{4} \end{aligned}\right\} \tag{16}$$

Derivation of **Eq. 15** to find $\theta(x,t,\tau)$, $M(x,t,\tau)$, $Q(x,t,\tau)$, and write them in matrix form:

$$\begin{Bmatrix} y(x,t,\tau) \\ \theta(x,t,\tau) \\ M(x,t,\tau) \\ Q(x,t,\tau) \end{Bmatrix} = \begin{bmatrix} A & B & -C & -D \\ -4\alpha D & \alpha A & -\alpha B & -\alpha C \\ E_sI_s\cdot 4\alpha^2 C & E_sI_s\cdot 4\alpha^2 D & E_sI_s\cdot\alpha^2 A & E_sI_s\cdot\alpha^2 B \\ E_sI_s\cdot 4\alpha^3 B & E_sI_s\cdot 4\alpha^3 C & -E_sI_s\cdot 4\alpha^3 D & E_sI_s\cdot\alpha^3 A \end{bmatrix} \times \begin{Bmatrix} y_0(t,\tau) \\ \frac{\varphi_0(t,\tau)}{\alpha} \\ \frac{M_0(t,\tau)}{\alpha^2\cdot E_sI_s} \\ \frac{Q_0(t,\tau)}{\alpha^3\cdot E_sI_s} \end{Bmatrix} \tag{17}$$

Substitute the four boundary conditions of **Eq. 11** again to obtain the initial parameters $y_0(t,\tau)$ and $M_0(t,\tau)$:

$$\left.\begin{aligned} y_0(t,\tau) &= \frac{P}{\alpha^3 E_sI_s\dfrac{C^2(\alpha h_s) - B(\alpha h_s)D(\alpha h_s)}{A(\alpha h_s)B(\alpha h_s) + 4C(\alpha h_s)D(\alpha h_s)}} \\ M_0(t,\tau) &= \frac{P}{\alpha}\cdot\frac{4D^2(\alpha h_s) + A(\alpha h_s)C(\alpha h_s)}{A(\alpha h_s)B(\alpha h_s) + 4C(\alpha h_s)D(\alpha h_s)} \end{aligned}\right\} \tag{18}$$

The time-dependent shear stiffness of SSC is:

$$\begin{aligned} K_s(t,\tau) &= \frac{P}{y_0(t,\tau)} \\ &= E_sI_s\left[\frac{k(t,\tau)}{4E_sI_s}\right]^{3/4}\frac{A(\alpha h_s)B(\alpha h_s) + 4C(\alpha h_s)D(\alpha h_s)}{C^2(\alpha h_s) - B(\alpha h_s)D(\alpha h_s)} \\ &= [k(t,\tau)]^{3/4}E_s^{1/4}d_s\cdot Z_m \end{aligned} \tag{19}$$

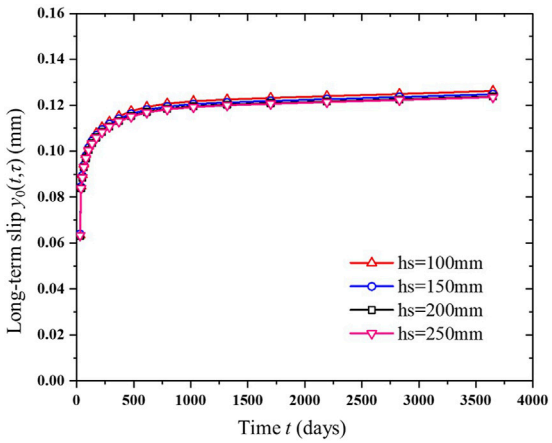


**FIGURE 5 |** Time dependent relative slip with increasing stud height.

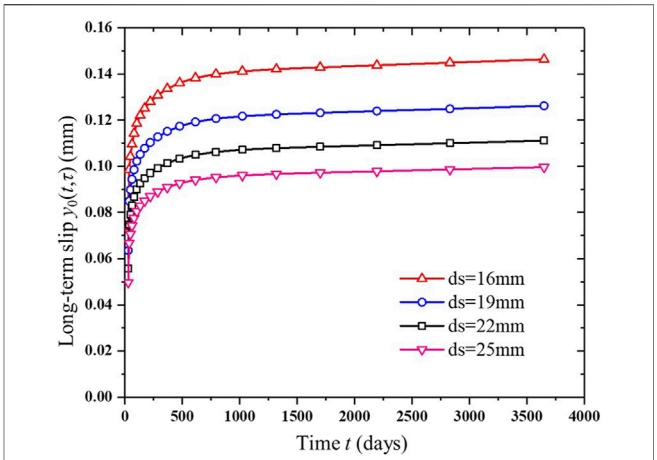


**FIGURE 7 |** Time dependent relative slip with increasing stud diameter.

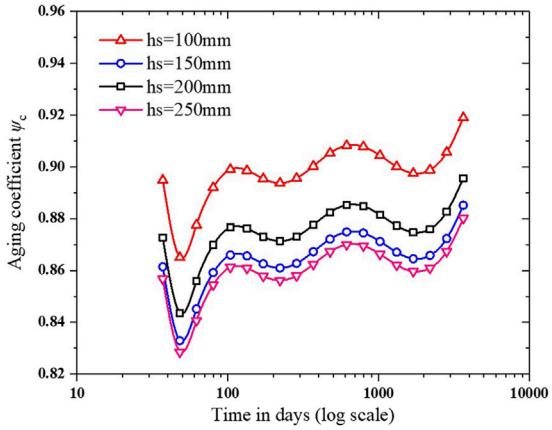


**FIGURE 6 |** Aging coefficient with increasing stud height.

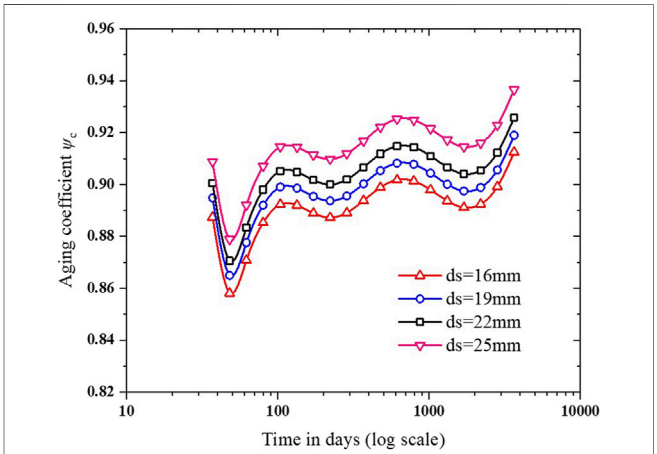


**FIGURE 8 |** Aging coefficient with increasing stud diameter.

In **Eq. 19**, $Z_m$ is a simplified coefficient term. When $\alpha h_s \geq 3$, its value is little affected by the change of $\alpha h_s$, and it is considered to be constant. **Equation 19** is further simplified into the form of reducing the initial shear stiffness $K_{ini}$ $(\tau)$ of SSC,

$$K_s(t,\tau) = \left[\frac{k(t,\tau)}{1+\psi_c(t,\tau)\varphi_c(t,\tau)}\right]^{3/4}$$
$$E_s^{1/4} d_s Z_m = \frac{K_{ini}(\tau)}{\left[1+\psi_c(t,\tau)\varphi_c(t,\tau)\right]^{0.75}} \quad (20)$$

In **Eq. 20**, $\psi_c$ $(t, \tau)$ is the aging coefficient of concrete, which is determined by back calculation based on the results of tests or solid finite element calculations; $\varphi_c$ $(t, \tau)$ is the creep coefficient of concrete, calculated by using the creep model recommended by the code; $K_{ini}$ $(\tau)$ is the initial shear stiffness of SSC, and it can be determined by **Eq. 21**.

$$K_{ini}(\tau) = [k(t,\tau)]^{0.75} E_s^{0.25} d_s Z_m \quad (21)$$

Gilbert and Bradford (1991) put forward the expression of the concrete foundation constant $k$ $(\tau)$ at the initial stage of loading,

$$k(\tau) = \frac{E_c(\tau)}{\beta} \quad (22)$$

In **Eq. 22**, $E_c$ $(\tau)$ is the initial elastic modulus of concrete; $\beta$ is the factor of the ratio function of welding stud diameter and spacing, and its range is between 2.5 and 3.3, regardless of age. Substitute **Eq. 22** into **Eq. 21**, simplify to get **Eq. 23**.

$$K_{ini}(\tau) = E_c^{0.75} E_s^{0.25} d_s \cdot c \quad (23)$$

In **Eq. 23**, $c$ is the simplification coefficient which is determined according to the back calculation of the initial shear stiffness test data of SSC. Lin et al. (2014) calculated the initial shear stiffness of SSCs based on the shear push-out test data of 99 SSCs, and calculated the initial shear stiffness of SSCs by taking the slope of the secant line of the shear force-slip curve corresponding to the slip of 0.2 mm, and the linear regression obtained $c$ was 0.32.

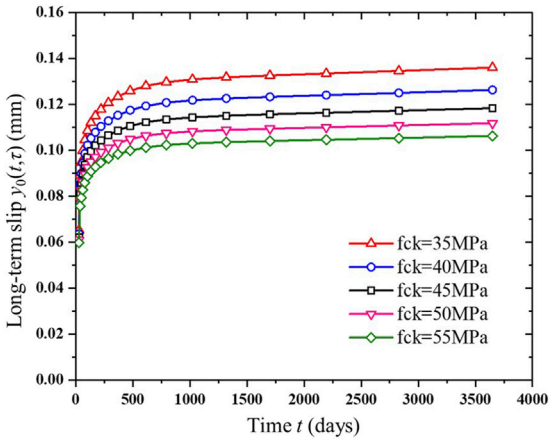


**FIGURE 9 |** Time dependent relative slip with increasing concrete strength.

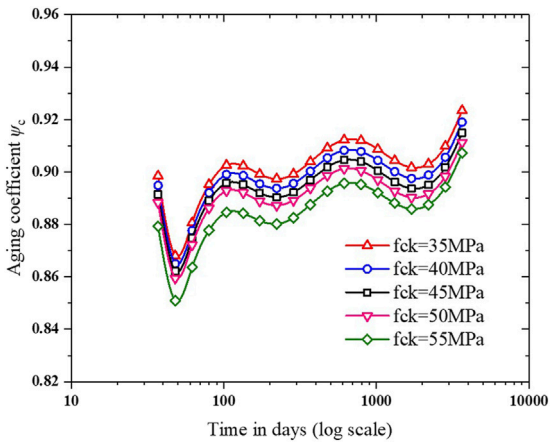


**FIGURE 10 |** Aging coefficient with increasing concrete strength.

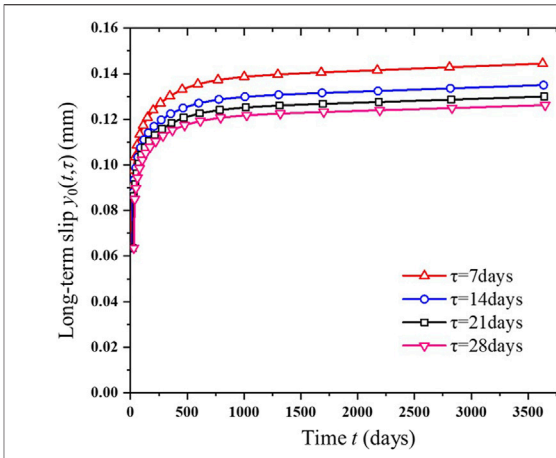


**FIGURE 11 |** Time dependent relative slip with increasing loading age.

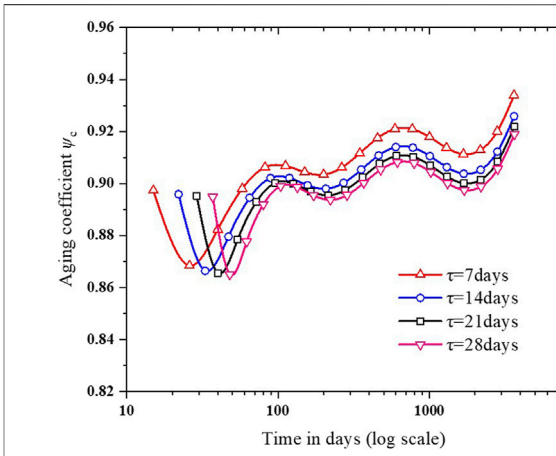


**FIGURE 12 |** Aging coefficient with increasing loading age.

## VERIFICATION OF ANALYTICAL RESULTS

At present, there are few experimental data on the time-dependent behavior of welding studs, and most of them are analyzed based on solid finite element models. In this paper, a solid finite element model is established by taking the shear push-out test of a welding stud connector with a diameter ds of 19 mm and a height of $h_s$ of 100 mm as an example. The push-out specimens include concrete blocks, 310UB40 I-shaped steel members (AS, 2010), SSC and reinforcement with a diameter of 12 mm. The detailed dimensions of the specimens are shown in **Figure 3**. Both concrete and steel are considered as linear elastic materials. The cylindrical compressive strength of concrete is $f_{ck}$ = 40 MPa, the initial elastic modulus $E_c$ = 36268 MPa, and the steel elastic modulus $E_s$ = 200 GPa. On the 29th day after the concrete was poured, a load of 130 kN was continuously applied on the top of the steel member, and the shear force $P$ obtained by the even distribution of the root of each welding stud was 32.5 kN. The average relative humidity of the environment is 70%. The fib MC 2010 creep model is used to calculate the creep coefficient, and the concrete creep coefficient $\varphi_c$ (3650, 29) is about 1.629 when the loading age is 10 years. The creep effect is calculated by the step-by-step method (SSM) with improved precision (Liu et al., 2021). The whole creep process is divided into 20 steps. The slip measurement points of steel and concrete on the interface are shown in **Figure 3**, and the average relative slip of the upper and lower SSC is taken as the relative slip of the interface.

**Figure 4A** shows the comparison between the theoretical value of the interface long-term slip which is calculated by **Eq. 20** proposed by the author and the calculated value of FEA. When the concrete aging coefficient $\psi_c$ takes different values, the long-term interface slip will change accordingly. When $\psi_c$ is set to 0.9, the theoretical value of interface slip at different ages is highly consistent with the calculated value of FE. **Figure 4B** shows the comparison between the theoretical value of the interface long-term slip which is calculated by **Eq. 1** proposed by Al-Deen et al. (2011) and the calculated value of FEA. Since the model in this paper uses C40 concrete, its elastic modulus and creep coefficient are the same as those of Al-deen. Compared with the Al-deen test, if $\alpha_{sc}$ is set as 0.4, there will be a large deviation from the FE value. When $\alpha_{sc}$ increases,

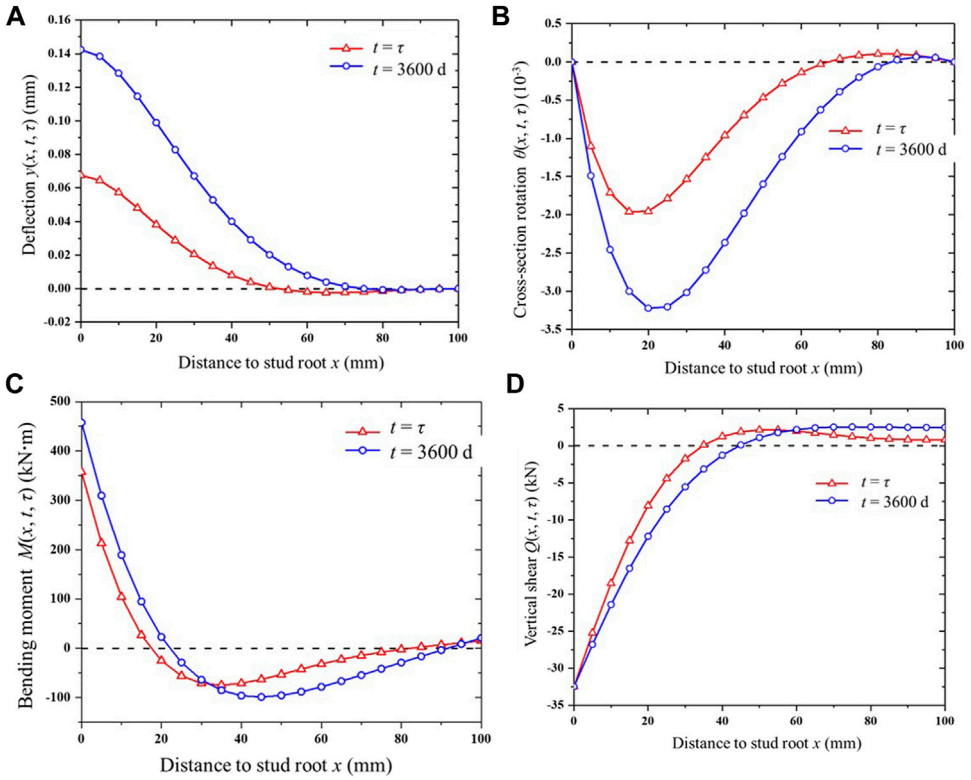


**FIGURE 13 |** Time-dependent response of the beam on elastic foundation.

the theoretical value of interfacial long-term slip gets closer to the calculated value of FE. When $\alpha_{sc}$ is set to 0.8, the theoretical value of interface slip is basically consistent with the calculated value of FE. Using the equations proposed in this paper or by Al-Deen et al. (2011) to determine the time-dependent shear stiffness of SSC, the theoretical results is probably close to the FE result if appropriate $\psi_c$ or $\alpha_{sc}$ are selected. It is crucial to determine the appropriate value of $\psi_c$ considering the geometric parameters of SSC, concrete strength and the different stud sizes, concrete strengths and creep coefficients.

## PARAMETRIC STUDY

The aging coefficient reflects the influence of concrete aging on the creep deformation, and is closely related to the creep coefficient and the complex stress state of the concrete on the pore wall. Bazant (1972) gave the expression of aging coefficient when deriving the simplified calculation method of concrete creep AEMM:

$$\psi_c(t,\tau) = \left[1 - \frac{E_R(t,\tau)}{E_c(\tau)}\right]^{-1} - \frac{1}{\varphi_c(t,\tau)} \tag{24}$$

In **Eq. 24**, $E_R$ (t, τ) is the relaxation function, that is, the stress at age $t$ is caused by applying unit strain at age $\tau$. In this part, the finite element model of the test entity based on the shear resistance of SSC is discussed, and the influence of the design parameters such as the diameter ds of SSC, the height $h_s$, the concrete strength $f_{ck}$, the concrete loading age $\tau$, the creep duration $t$—$\tau$ and other design parameters on $\psi_c$ ($t$, $\tau$) effect.

### Effects of Stud Height

The comparison of the effect of different welding stud heights on the long-term relative slip of the interface is shown in **Figure 5**. SSC height $h_s$ is selected between 100 and 250 mm, and it can be seen that SSC height has little effect on the interface relative slip. **Figure 6** shows the effect of the height of SSC on the aging coefficient of concrete. The aging coefficient $\psi_c$ is obtained by inverse calculation from the finite element calculation value of the relative slip of the interface. The change of the relative slip of the interface is highly sensitive to the value of $\psi_c$. As the height of SSC increases, $\psi_c$ decreases overall, and the rate of change of $\psi_c$ also decreases. The $\psi_c$ value of creep for 10 years is 0.919, 0.885, 0.896, 0.880 with the increase of welding stud height.

### Effects of Stud Diameter

The comparison of the effect of different welding stud diameters on the long-term relative slip of the interface is shown in **Figure 7**. The diameter of SSC ds is selected between 16 and 25 mm. It can be seen that the diameter of SSC has an effect on the relative slip of the interface, which is manifested in the interface slippage at the initial stage of loading. The slip decreases with increasing stud diameter, and the interface slip changes accordingly during creep. **Figure 8** shows the effect of welding stud diameter on concrete aging coefficient $\psi_c$. The

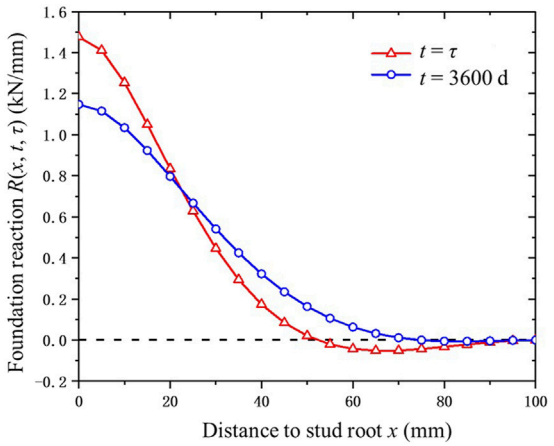


**FIGURE 14 |** Time-dependent reaction force of the foundation.

value of $\psi_c$ increases with the increase of the diameter of SSC. The $\psi_c$ value of creep for 10 years is 0.912, 0.919, 0.926, and 0.937 with the increase of the diameter of SSC.

### Effects of Concrete Strength

The comparison of the effects of different compressive strengths of concrete on the long-term relative slip of the interface is shown in **Figure 9**. The compressive strength $f_{ck}$ of concrete is between 35 and 55 MPa. At the initial stage of loading, as the strength of concrete increases, the modulus of the foundation increases, the deformation of SSC decreases, and the corresponding interface relative slip also decreases. During the creep period, the creep coefficient of C55 concrete is smaller than that of other low-strength concrete, and the slip of SSC is the smallest at the end of creep. **Figure 10** shows the effect of concrete strength on the aging coefficient $\psi_c$. The value of $\psi_c$ decreases with the increase of concrete strength. The $\psi_c$ value of creep for 10 years is 0.923, 0.919, 0.915, 0.911, and 0.907 in turn with the increase of concrete strength.

### Effects of Loading Age

The comparison of the effect of concrete loading age on the long-term relative slip of the interface is shown in **Figure 11**. The loading age τ is between 7 and 29 days. The relative slip of the interface at the initial stage of loading is almost the same. During the creep period, the creep coefficient of concrete decreases with the increase of the loading age, and the corresponding creep slip increment also decreases. Slippage is minimal. **Figure 12** shows the effect of concrete loading age on the aging coefficient $\psi_c$. The $\psi_c$ value decreases with the increase of the loading age, and the $\psi_c$ value of the 10-year creep is 0.934, 0.926, 0.922, and 0.919 with the increase of the loading age.

## TIME-DEPENDENT RESPONSE OF STUD SHEAR CONNECTOR

In the process of using the elastic foundation beam theory to derive the time-dependent shear stiffness of SSC, the theoretical analytical equations for the beam deformation and the distribution of the internal force along the beam length are also given. Qualitative analysis of the deformation and internal force of the beam with a loading age of 29 days and a creep end of 10 years is shown in **Figure 13**. The deflection of the beam at the end of creep is larger than that at the initial stage of loading, and the bending moment of the root section increases, but the shear force remains constant.

**Figure 14** shows the distribution of the concrete foundation reaction force $R$ along the beam length. The distribution concentration of the foundation reaction force at the end of creep is gentler than that at the initial stage of loading. The length of the reaction force distribution along the beam length increases, and the foundation reaction force is redistributed. The conclusions drawn from the above theoretical analysis are basically consistent with the conclusions drawn from the solid finite element analysis of SSC, indicating that the effect of concrete creep on beam deformation and internal force can be simply predicted by the elastic foundation beam theory.

## CONCLUSION

Based on the viscoelastic foundation beam theory, this paper conducts a theoretical study on the time-dependent shear stiffness of SSC, and draws the following conclusions:

1) The analytical solution based on the theory of the beam on viscoelastic foundation may represent the long-term relative deformation of SSC under sustained loads.
2) The approximation of TDS for SSC may result in close prediction of long-term slip compared with the refined FEA. The proposed method maybe used for simplified evaluation of composite steel construction where the time-dependent partial interaction is of interest.
3) For a standard cure of SSC with 28 days of loading age, which is close to the construction of composite beam bridges, the 10-years-aging coefficient $\psi_c$ is suggested to be 0.88–0.95.

## DATA AVAILABILITY STATEMENT

The original contributions presented in the study are included in the article/supplementary material, further inquiries can be directed to the corresponding author.

## AUTHOR CONTRIBUTIONS

RL contributed to the idea, data collection, analysis, writing, review, revision and funding; XS contributed to the writing, review and revision; HY contributed to the idea, data collection, analysis, writing; YL contributed to the idea, reviw and funding.

## FUNDING

The research reported herein has been carried out as part of the research projects granted by the National Natural Science Foundation of China (51978245).

## REFERENCES


AASHTO (American Association of State Highway and Transportation Officials) (2012). *AASHTO LRFD Bridge Design Specifications*. 5th edition. USA: American Association of State Highway and Transportation Officials.

Akao, S., Kurita, A., and Hiragi, H. (1987). Effect of Directions of Concrete Placing on Behavior of Headed Stud Shear Connectors in Push-Out Tests. *Dob. Gakkai Ronbunshu* 1987, 311–320. doi:10.2208/jscej.1987.380_311

Al-Deen, S., Ranzi, G., and Vrcelj, Z. (2011). Full-Scale Long-Term Experiments of Simply Supported Composite Beams with Solid Slabs. *J. Constr. Steel Res.* 67, 308–321. doi:10.1016/j.jcsr.2010.11.001

AS (Australian/New Zealand Standard) (2010). *Structural Steel Part I: Hot-Rolled Bars and Sections*. 3rd edition. Sydney: Standards Australia. AS/NZS 3679.1: 2010.

Ban, H., Uy, B., Pathirana, S. W., Henderson, I., Mirza, O., and Zhu, X. (2015). Time-Dependent Behaviour of Composite Beams with Blind Bolts under Sustained Loads. *J. Constr. Steel Res.* 112, 196–207. doi:10.1016/j.jcsr.2015.05.004

Bazant, Z. P. (1972). Prediction of Concrete Creep Effects Using Age-Adjusted Effective. *J. Am. Concr. Inst.* 69, 212–217.

Bradford, M. A., and Gilbert, R. I. (1991). Time-Dependent Behaviour of Simply-Supported Steel-Concrete Composite Beams. *Mag. Concr. Res.* 43, 265–274. doi:10.1680/macr.1991.43.157.265

Gelfi, P., and Giuriani, E. (1987). Shear Force-Slip Relationship for Stud Connectors. Studi e Ricerche. *Corso di Perfezionamento per le Costruzioni Cem. Armato F. lli Pesenti* 9.

Hetenyi, M. (1958). *Beams on Elastic Foundation: Theory with Applications in the Fields of Civil and Mechanical Engineering*. Ann Arbor: University of Michigan Press. doi:10.1107/S0365110X59003103

Lin, Z., Liu, Y., and He, J. (2014). Research on Calculation Method of Shear Stiffness for Headed Stud Connectors. *Eng. Mech.* 6. (in Chinese). doi:10.6052/j.issn.1000-4750.2013.01.0034

Liu, R., Feng, Z., Ye, H., and Liu, Y. (2020a). Stress Redistribution of Headed Stud Connectors Subjected to Constant Shear Force. *Int. J. Steel Struct.* 20, 436–451. doi:10.1007/s13296-019-00295-3

Liu, R., Ye, H., Liu, Y., Zhao, H., Correia, J. A. F. O., and Xin, H. (2021). Numerical Simulation of Concrete Creep Behaviour Using Integral Creep Algorithm with Alternating Stresses. *Structures* 29, 1979–1987. doi:10.1016/j.istruc.2020.11.081

Liu, R., Ye, H., Zhao, H., and Liu, Y. (2020c). "Creep Effects of Perforated Rib Shear Connectors under Sustained Push-Out Load," in Concrete structures for resilient society - Proceedings of the fib Symposium 2020, 804-811. International fib Symposium on Concrete structures for resilient society, Shanghai, November 22, 2020 - November 24, 2020 (China: FIB International).

Liu, R., Zhao, H., Feng, Z., Xin, H., and Liu, Y. (2020b). Fatigue Evaluation on Headed Stud Connectors with Toe-Plate Failure Mode Using Hot Spot Stress Approach. *Eng. Fail. Anal.* 117, 104972. doi:10.1016/j.engfailanal.2020.104972

Mirza, O., and Uy, B. (2010). Finite Element Model for the Long-Term Behaviour of Composite Steel-Concrete Push Tests. *Steel & Compos. Struct.* 10, 45–67. doi:10.12989/scs.2010.10.1.045

Slutter, R. G. (1966). *The Fatigue Strength of Shear Connectors in Steel-Concrete Composite Beams*. Order No. 6704878. Bethlehem: Lehigh University. Available at: https://digital.lib.lehigh.edu/fritz/pdf/316_9.pdf.

Winkler, E. (1867). *Die Lehre von der Elasticitaet und Festigkeit besonderer Rucksicht auf ihre Anwendung in der Technik Fur politechniche Schulen, Bauakademien, Ingenieure, Maschinenbauer, architecten, etc*. Prag: H. Dominicus.

Xu, X., and Liu, Y. (2016). Analytical and Numerical Study of the Shear Stiffness of Rubber-Sleeved Stud. *J. Constr. Steel Res.* 123, 68–78. doi:10.1016/j.jcsr.2016.04.020

Xue, W., Ding, M., Wang, H., and Luo, Z. (2008). Static Behavior and Theoretical Model of Stud Shear Connectors. *J. Bridge Eng.* 1313, 6236–6634. doi:10.1061/(ASCE)1084-0702

Zheng, S., and Liu, Y. (2014). Experiment of Initial Shear Stiffness of Perfobond Connector. *China J. Highw. Transp.* 27, 7. (in Chinese). doi:10.19721/j.cnki.1001-7372.2014.11.010


**Conflict of Interest:** The authors declare that the research was conducted in the absence of any commercial or financial relationships that could be construed as a potential conflict of interest.